



Contents lists available at ScienceDirect

International Journal of Solids and Structures

journal homepage: www.elsevier.com/locate/ijsolstr

Role of cell regularity and relative density on elasto-plastic compression response of random honeycombs generated using Voronoi diagrams

Oscar E. Sotomayor, Hareesh V. Tippur*

Department of Mechanical Engineering, Auburn University, AL 36849, United States

ARTICLE INFO

Article history:

Received 9 November 2013

Received in revised form 13 February 2014

Available online xxxx

Keywords:

Cellular solids

Voronoi diagrams

Virtual design

Cell regularity

Compression

Elasto-plastic analysis

Finite elements

ABSTRACT

The Voronoi tessellation technique and solid modeling methods are used in this work to create virtual random structures and link cell morphology with the mechanical behavior. Their compression responses are analyzed using the finite element method. First, the effect of loading direction is analyzed for structures with different levels of randomness characterized by a regularity parameter to assess the degree of scatter in the results. Subsequently, morphological characteristics such as arrangement of cells and randomness are analyzed separately. The effect of relative density on structures with different levels of randomness is also studied. Simulations suggest that at low relative densities the arrangement of cells has a negligible effect on the compression response of random honeycombs. On the contrary, the cellular randomness has significant influence on the elastic and plastic characteristics especially when fully random structures are compared with the regular counterparts.

© 2014 Elsevier Ltd. All rights reserved.

1. Introduction

Honeycombs, natural or man-made, are cellular solids whose geometry does not vary considerably in one of the three orthogonal directions; hence, they can be analyzed in a 2D dimensional space. *Honeycombs can also be used to understand the limiting behaviors of more complex 3D structures such as foams.* Similar to other cellular solids, honeycombs have a low relative density, high strength-to-weight ratio and good energy absorption characteristics. While man-made honeycombs are generally fabricated using a regular arrangement of standard unit cells such as triangles, squares, rhombus, hexagons (most common), circles or other 2D geometries, natural honeycombs such as balsa wood tend to show non-uniformity and randomness (see for example [Da Silva and Kyriakides \(2007\)](#)). Hence, honeycombs could have non-repeatable and non-periodic cellular structure and as a consequence may have characteristics that are structurally advantageous. Techniques to create such random honeycombs on-demand and with a prescribed cellular morphology are also available at the moment. For instance, [Fig. 1\(a\)](#) shows an example of the CAD model of an irregular honeycomb with 314 cells along with the real structure produced using an additive manufacturing technique. Specifically, the Voronoi

honeycomb model shown in [Fig. 1](#) was produced by the authors using Polyjet Technology¹ and VeroWhitePlus® material. Conceivably, such capabilities could be useful in producing bio-scaffolds for tissue generation ([Liu et al., 2007](#)) or lightweight prosthetics.

A Voronoi honeycomb can be created using the Voronoi tessellation technique to divide 2D space based on random generation of nuclei. The criterion used for the division of space is association of all the locations in the 2D space with the nearest nucleus. The Voronoi tessellation technique can be extended from 2D to 3D to form more complex microstructures such as the ones seen in structural foams to help understand the relationship between cellular morphology of foams and their mechanical properties. For example, [Gaitanaros et al. \(2012\)](#) used the Voronoi tessellation technique and the Surface Evolver software package to generate virtual designs that closely resemble the microstructure of random foams at a constant level of randomness. It is widely shown that the mechanical response of honeycombs depend primarily on the base material characteristics, relative density $\bar{\rho}$ (density of the cellular solid to the density of the bulk material (ρ^*/ρ_s)) and honeycomb morphology. [Gibson and Ashby \(1997\)](#) have studied the influence of relative density on the compression response of regular hexagonal honeycombs. By making use of bending theory they have shown that

* Corresponding author. Tel.: +1 334 844 3327.

E-mail address: tippuhv@auburn.edu (H.V. Tippur).

¹ In a Polyjet Technology, a thin layer of photopolymer in the liquid state is injected or sprayed over a build-tray followed UV radiation to cure the polymer. The build-tray moves down incrementally and the computer controlled process is repeated according to a CAD model.

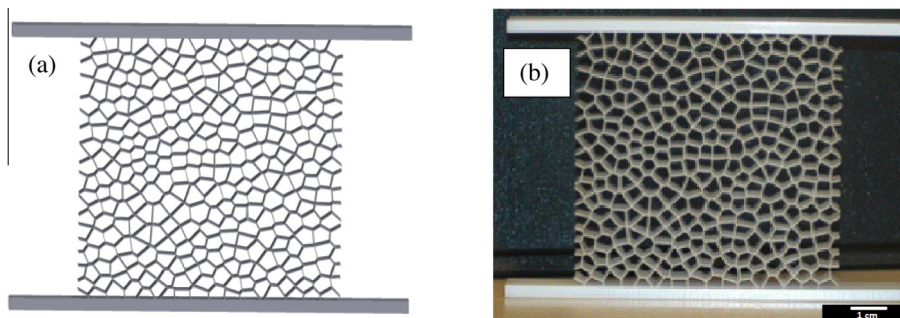


Fig. 1. Voronoi honeycomb with 314 cells: (a) CAD model, (b) real specimen. Produced with a Polyjet Technology in VeroWhitePlus[®] material.

the elastic modulus and strength of regular hexagonal honeycombs scale with $\bar{\rho}^3$ and $\bar{\rho}^2$, respectively, at low relative densities. Indeed, a regular hexagonal honeycomb can be considered as a particular case of a Voronoi (or, irregular) honeycomb in which the cell nuclei are perfectly ordered in a rhombic arrangement.

Simulation of honeycombs using FE methods can be performed using a unit cell and periodic boundary conditions when the honeycomb has a uniform repeating pattern. In an effort to better represent the morphology of 2D foams and simulate their mechanical response, a few investigators in the past (Alkhader and Vural, 2008; Silva and Gibson, 1997; Tekoglu et al., 2011) have applied the 2D Voronoi tessellation technique in conjunction with FE methods. However, to date, most reports focus on the influence of relative density and cell size on the mechanical response of foams. And, there is a lack of research on the role of cell regularity (or, irregularity) on the mechanical performance of honeycombs and foams. Furthermore, the regularity parameter is rarely identified when the Voronoi tessellation technique is applied to represent foams virtually even though it has a rather strong effect on the final topology of honeycombs. The work of Alkhader and Vural (2008) is an exception and it addresses this issue for a limited range of cellular regularities. It should be noted that the effect of regularity on the compression response of Voronoi honeycombs with *linear elastic* base material characteristics is presented in Zhu et al. (2001, 2006).

In the present work, the effect of cell regularity on the compression response of honeycombs is studied over a wide range of regularities from fully random to ideally regular structures using Voronoi tessellation and finite element analysis. Gaining insight into potential failure responses of complex space filling 3D foams via these simpler 2D relatives motivates this study. Advances in additive manufacturing methods capable of producing random cellular structures and scaffolds with tailored functionalities such as gradations in cell wall thickness and/or material, and cell size also add to the motivation. Unlike the previous works which study the effect of regularity on the compression response of Voronoi honeycombs by modeling the base material as a linear elastic solid or elastic-perfectly plastic base material, in this work they are modeled with an elasto-plastic with a bilinear hardening response (approximating the commercially available AL-6061-T6). Additionally, the effect of cell regularity on the compression response of Voronoi honeycombs is studied for different relative densities. Furthermore, the effect of the *arrangement* of cells which is a concept different from that of regularity is also analyzed.

2. Solid modeling

2.1. Voronoi diagrams

By having a set of n nuclei representing the centers of bubbles growing in a m -dimensional Euclidean space, the Voronoi tessellation technique can be used to link all the points in that

space with the nearest nucleus (Klein, 1989; Moller, 1994; Okabe et al., 1945). This generates n regions that form the so-called Voronoi diagram. In this work, such a division of space has been implemented in Matlab[®] using the Qhull algorithm (Barber et al., 1996).² The Voronoi diagram represents the limiting case of growing bubbles in space under the assumption that (i) bubbles nucleate simultaneously in a determinate region of space, (ii) nuclei of the bubbles stay in fixed positions during growth, (iii) the rate of growth is constant in all directions, and (iv) the growth is interrupted when bubbles touch the adjacent ones (Boots, 1982; Silva et al., 1995; Tekoglu et al., 2011). The Voronoi diagram being unique for a given set of points, the shape of the diagram can be controlled by generating different arrangement (or distribution) of nuclei (see, Klein (1989), Moller (1994), Okabe et al. (1945)). For the case of monodispersed nuclei, a fully regular pattern of points generates regular Voronoi diagram whereas an irregular pattern leads to a random counterpart. Natural honeycombs may not be always fully irregular or regular and hence their configuration can be viewed as somewhere in between these two limits.

2.2. Regularity parameter

A pseudo-random arrangement of points can be generated using a Poisson probability distribution if (i) the points are generated independently from the previous ones, (ii) the probability of a nucleus to be generated in a region of space is proportional to the size of the region, and (iii) the probability of two nuclei generated at the same location is negligible (Martinez and Martinez, 2002; Okabe et al., 1945). As mentioned previously, a fully random Voronoi honeycomb generated with a Poisson probability distribution does not fully represent the morphological characteristics observed in natural honeycombs (Gibson and Ashby, 1997). For example, the range of cell sizes generated with a fully random arrangement of nuclei is too broad when compared to natural honeycombs. To address this, it is often necessary to increase the regularity of the nuclei by eliminating points that are closer than a certain predetermined (prescribed) distance called the *distance of inhibition* (s). In this work, a Simple Sequential Inhibition (SSI) algorithm in Matlab[®] (Martinez and Martinez, 2002) is used to accomplish this task. In a SSI process, a set of points are randomly generated one at a time based on a Poisson probability distribution. Subsequently, the point is eliminated if the distance from the previously generated ones is less than a prescribed distance of inhibition (s) (Martinez and Martinez, 2002; Okabe et al., 1945). The maximum possible value of the distance of inhibition is a function of the size of the 2D region and the number of points to be generated. Zhu et al. (2001) presented an expression for calculating the maximum distance of inhibition (r) in a 2D space as,

² Initially developed at the Geometry Center of the University of Minnesota, Minneapolis, MN.

$$r = \sqrt{\frac{2A}{\sqrt{3}n}} \quad (1)$$

In the above equation, A is the control area where n nuclei are located. Therefore, the regularity parameter can be quantified with s or by using a ratio of s to the maximum value of r (see Zhu et al. (2000, 2001) and references therein) as,

$$\delta = \frac{s}{r} \quad (2)$$

In the present work, δ will be referred to as the regularity parameter or simply “regularity”. Fig. 2 illustrates an example of the effect of increasing the regularity parameter, for say $n = 314$ nuclei. A value of $\delta = 1$ implies a regular arrangement of points maintaining a maximum distance of inhibition among them (see, Fig. 2(e)) whereas a regularity parameter of $\delta = 0$ represents a completely random arrangement of points (as in Fig. 2(a)). As evident in Fig. 2, the cell size distribution varies with the regularity parameter. While the size of the cells is uniform for the $\delta = 1$ case, the largest difference between cell sizes is for $\delta = 0$. Indeed, the biggest cell is almost 30 times the smallest one when $\delta = 0$. The number of faces per cell is also affected by the regularity parameter. That is, the probability of finding cells with six sides ($F=6$) in a regular 2D Voronoi honeycomb is equal to 1 whereas the probability is lower in case of irregular counterparts. Fig. 3 shows the probability of finding cells with F faces for the geometries presented in Fig. 2. Note that the trivial case of $\delta = 1$ is not presented in Fig. 3. While only six sided polygons can be found in case of $\delta = 1$, a few sided polygons up to nine sides are present when $\delta = 0$. However, a six sided polygon, as Euler’s law requires, is still the most probable polygon in all configurations. It is worth noting that the six-sided polygons are also the most common ones in natural honeycombs.

Under the assumption that a certain number of nuclei can be generated in a region for a minimum distance of inhibition, the computational time for the SSI process to generate the nuclei depends on the regularity parameter and the computational resources available. While it may take only a few seconds to generate a fully random arrangement of nuclei, the computational

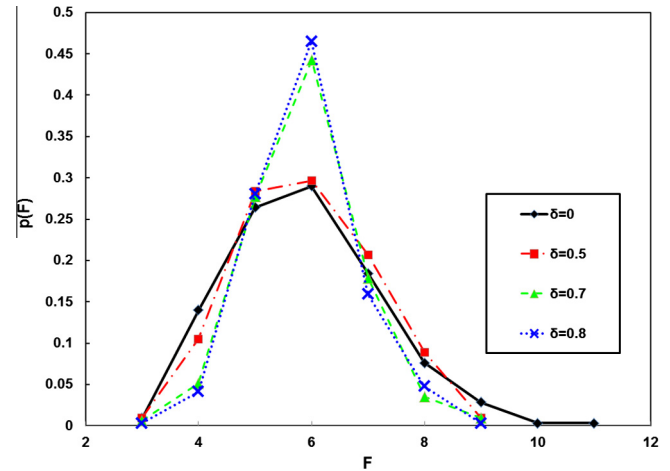


Fig. 3. Probability $p(F)$ of finding cells with F faces with different levels of regularity in Voronoi diagrams shown in Fig. 2. (The trivial case of regular honeycomb ($F=6$) is not shown.)

time for a random process (SSI) to generate a regular output is theoretically infinity according to the probability theory for large numbers (see Borel (1913)). Hence, in this work, the nuclei of the regular arrangement of points in 2D (see Fig. 2(e)) were directly located in regular positions using the r value without resorting to random generation of points.

2.3. Construction of 2D geometries

Matlab[®] was used for dividing space in accordance with the Voronoi tessellation technique whereas AutoCAD was employed for constructing 2D geometries. Four characteristics, namely, (i) size of the model, (ii) regularity, (iii) cross sectional shape, and (iv) relative density, were defined while generating planar monodisperse Voronoi geometries. First, the size of the model (that is, the number of cells) was chosen to be sufficiently large in order

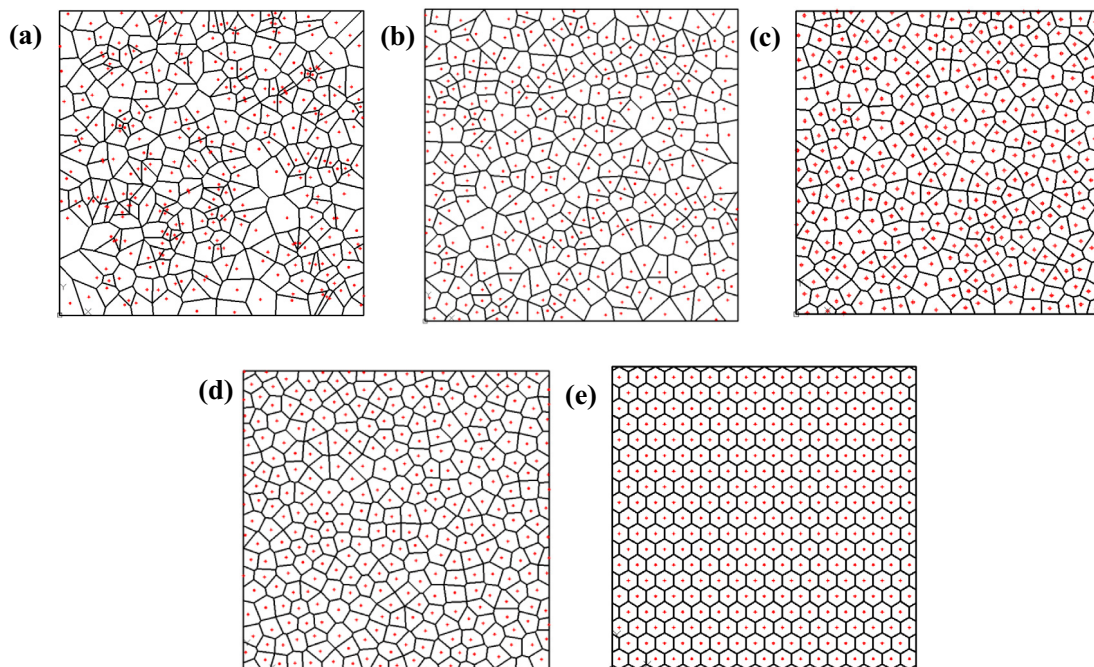


Fig. 2. Voronoi diagrams and the nuclei (dots) used for generating honeycombs with $n = 314$ and (a) $\delta = 0$, (b) $\delta = 0.5$, (c) $\delta = 0.7$, (d) $\delta = 0.8$, (e) $\delta = 1$.

to represent a continuum foam model while keeping the size of the model small enough to be able to manage it using the available solid modeling and FE software resources. A few previous studies analyze the effects of the model size on the compression response of Voronoi honeycombs. For the 2D case, Tekoglu et al. (2011) have shown that for uniaxial compression a ratio of the control area to the cell size of greater than or equal to 16 produces tolerable elastic modulus and plastic collapse strength variations. Hence, the *plastic collapse strength* is defined as the maximum strength reached in the stress–strain curve before collapse and reaching a stable *plateau stress*. A similar assertion has been made by Alkhalid and Vural (2008) by showing that 10–15 cells in the loading direction produce convergence in elastic modulus and crushing stress. Accordingly, in this work, a control area corresponding to a ratio of the area to cell size equal to approximately 16 was selected. The choice was further validated by an independent convergence study, presented in Appendix A. For an arrangement of nuclei in a regular (hexagonal) honeycomb, this corresponds to $n = 314$ cells. Second, in order to study the effect of cell regularity over the complete range, from to $\delta = 1$, Voronoi honeycombs with $n = 314$ cells and regularity $\delta = \{0, 0.5, 0.7, 0.8 \text{ and } 1\}$ were generated. Regarding the cross-sectional shape of the ligaments, Gong and Kyriakides (2005), Gong et al. (2005), Jang et al. (2008), Jang and Kyriakides (2009) studied the morphology of open-cell aluminum foams by means of micro-computed X-ray tomography. They observed that the cross-sectional shape of the ligaments were in between a triangle and a circle. In the present work, for simplicity, the cross-sectional shape of the ligaments was modeled with a constant circular cross-section. (Though unusual, this choice was to help compare the results with 3D Voronoi foam behavior under similar loading conditions and minimize the effect of the orientation of the cross section.) The accumulation of material at the junctions of ligaments, typical of structural 2D foam representations, has been modeled by overlapping cross-sections of beam elements. Additionally, the analysis has been limited to a relative density of up to $\bar{\rho} = 9\%$ to minimize this effect (see, Gan et al. (2005), Jang et al. (2008) and references therein). With these considerations, the value of the radius/thickness of struts depends on the relative density of the honeycomb. In 2D it can be calculated as (Liu et al., 2009; Tekoglu et al., 2011; Zhu et al., 2000),

$$\bar{\rho} = \left(\frac{1}{A}\right) \sum_{i=1}^N h_i l_i \quad (3)$$

where $\bar{\rho}$ is the relative density of the foam, N is the number of struts in the cell, h_i is the thickness of struts, l_i is the cell wall length and A is the control area. Additionally, considering that the open-cell aluminum foams are normally produced in the range of 3–12%, the analyses were limited to an upper value of 9%. Specifically, four relative densities $\bar{\rho} = \{3\%, 5\%, 7\% \text{ and } 9\%\}$ were analyzed in this work. Based on this, for a given value of A , the thickness of struts was calculated. Additionally, to study the compression response in the vertical direction (x_2), left and right borders of the control area were eliminated to emulate real foams compressed in a sandwich-like configuration with free ligaments on the lateral faces. Similarly, the top and bottom borders of the control area were eliminated when the compression response in the horizontal direction (x_1) was simulated.

3. Finite element modeling

Structural analysis of the foam models was performed using the finite element software package Abaqus/Standard (Hibbitt, 2002). In the pre-processing stage, geometries described in Section 2.3 were imported from AutoCAD into Abaqus®. The base material was modeled as an elasto-plastic material with a bilinear isotropic

hardening response corresponding to the reported stress–strain characteristic for AL-6101-T6 (Aluminum Association). Specifically, the elastic region was described by an elastic modulus of 68.9 GPa and a Poisson's ratio of 0.33 whereas the plastic region had an initial yield stress of 193 MPa and a slope of $\Delta\sigma/\Delta\epsilon = 149$ MPa up to a strain of 19%. Beyond that strain the stress was assumed constant at 221 MPa. Further, interactions among cell walls when large deformations occur play an important role in the overall mechanical response of the Voronoi honeycombs. If interactions between cells are not simulated correctly, interpenetration of elements can affect the results at higher strains. In view of this, surfaces were created in the interior of each closed cell at the mid-surface of the beam elements and frictionless interaction of the self-contact type was stipulated for these surfaces. (In reality, interactions between cells occur at the ligament surface instead of the mid-surface. However, the idealization was considered reasonably accurate for low relative densities.) Nonlinear effects due to large deformations were activated in a generalized static analysis performed in Abaqus/Standard. Moreover, convergence of unstable nonlinear problems was improved using an adaptive automatic stabilization scheme (Hibbitt, 2002; Jhaver, 2009). Values of 2×10^{-4} and 0.05 for dissipated energy fraction and ratio of stabilization energy to strain energy were used in this work.

When the response was studied for compression in the x_2 -direction, a displacement boundary condition was applied on the top surface while constraining the bottom surface from displacing in the x_2 -direction. Additionally, a point in the middle of top and bottom surfaces was constrained from displacing in the x_1 -direction. The boundary conditions were rotated by 90° when the compression response in the x_1 -direction was sought.

Beam elements with three active degrees of freedom per node and a quadratic interpolation within the domain were selected for FE discretization. The elements, identified as B22 in Abaqus®, are formulated on Timoshenko's beam theory to take into account shear deformations in addition to flexure, which could be significant in short beams. Typically five nodes per ligament were generated during discretization although the number of nodes in case of short ligaments was reduced to three. This was to avoid generation of extremely short elements unsuitable for capturing beam-like deformations (Silva et al., 1995). Computations were performed as a batch job in a parallel processing environment. The number of elements in a typical simulation was in the range of 1846–1906 and more than 10,000 degrees of freedom.

In the post-processing stage, reaction forces at the bottom surface were added in order to obtain the net reaction force (F). The apparent stress on the Voronoi honeycombs was calculated by dividing F by the area of the base (Silva and Gibson, 1997). The average strain was calculated by dividing the displacement by the original length in the loading direction. A comparable analysis was performed when the displacement was imposed in the x_1 -direction. All these calculations were accomplished for each load increment in order to get a relatively continuous mechanical response curves.

The response for the Voronoi honeycomb with a regularity of $\delta = 1$, $\bar{\rho} = 9\%$, loaded in the x_2 -direction is presented in Fig. 4. The figure also depicts deformed honeycomb structure at five points of interest. In Fig. 4, the stress–strain response of the regular honeycomb presents two characteristic regions. First, an elastic region with a uniform deformation at small strains can be observed in Fig. 4. Then, a change in the slope of the stress–strain variation without an appreciable or noticeable area of localization of deformation is seen in the response. The deformations start to localize at the center of the model causing a collapse of a horizontal row of cells until the opposing cell walls contact each other. This produces an oscillatory characteristic. Others have previously reported comparable behaviors in the literature as well (see, Cricri et al.

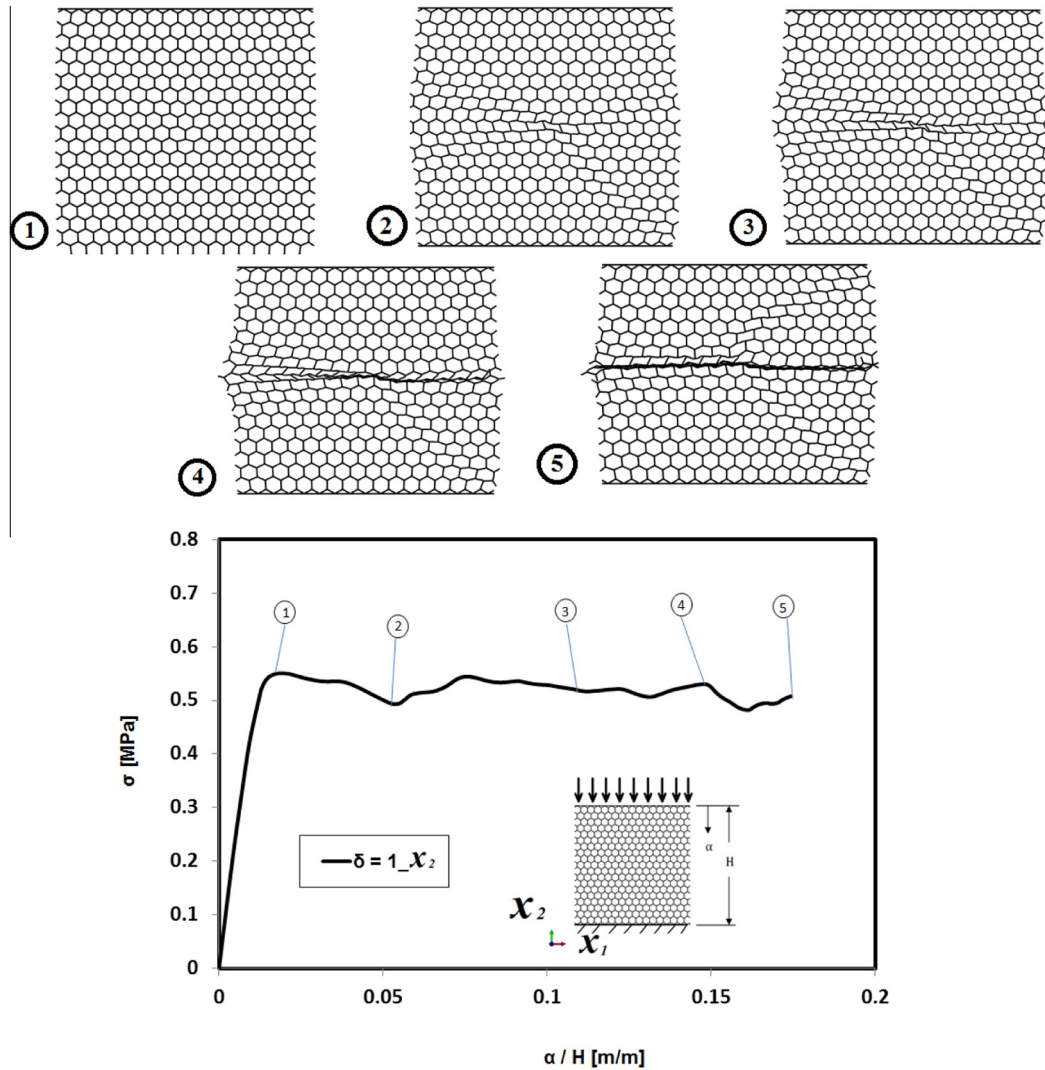


Fig. 4. Stress–strain curves for Al Voronoi honeycomb with a $\bar{\rho} = 9\%$, $\delta = 1$ loaded in the x_2 -direction.

(2013), Papka and Kyriakides (1994, 1998)). A good correlation between the current simulations and results available in literature in both the elastic and plastic regimes are observed for the regular honeycomb with $\bar{\rho} = 9\%$. Due to the fact that a hexagonal honeycomb can be considered as a particular case of a Voronoi honeycomb with $\delta = 1$, the validation process was assumed applicable to the rest of the regularities, namely, $\delta = \{0, 0.5, 0.7, 0.8\}$, as well

4. Voronoi honeycomb results

4.1. The effect of loading direction

In this section the effect of loading direction on the compression response of Voronoi honeycombs is examined. Even though random structures based on Voronoi diagrams are nominally isotropic when a sufficiently large number of cells are used in the simulation, studying of the loading direction helps to estimate the degree of scatter in the reported results. The stress has been normalized by the yield stress of the solid material (σ_{ys}) and the square of the relative density $\bar{\rho}^2$ in order to make the results broadly applicable. Hence, a reduced stress $\bar{\sigma}$ is defined as,

$$\bar{\sigma} = \frac{\sigma}{\sigma_{ys} \cdot \bar{\rho}^2}. \quad (4)$$

The term $\bar{\rho}^2$ is used in the normalization due to the fact that the strength is known to scale with $\bar{\rho}^2$ at low relative densities. For instance, the stress–strain response for the case of $\bar{\rho} = 9\%$ and $\delta = \{0.5 \text{ and } 0.8\}$ are shown in Figs. 5 and 6, respectively. Additionally, deformed Voronoi honeycomb configurations at five points of interest are also presented in those figures. The deformed configurations are identified with a number when compressed in the x_2 -direction and with a letter when compressed in the x_1 -direction. Regarding the elastic responses in Figs. 5 and 6, both the configurations exhibit a nearly linear variation and the elastic modulus depends on the degree of regularity δ . The variation in the elastic modulus for different relative densities and regularities is analyzed in Sections 4.3 and 4.4. In the present section, the focus is limited to the directional response of Voronoi honeycombs. As expected, the predicted elastic modulus is essentially independent of the loading direction due to the fact that we are dealing with isotropic configurations. A similar assertion can be made for the plastic collapse strength as well. The response in the plateau region oscillates about a mean level for the two orthogonal directions. The small variations are attributed to the random morphology of cells inherent to the construction process of generating the Voronoi geometries. The sequence of deformation in Figs. 5 and 6 present a behavior akin to the regular honeycomb case (Fig. 4). For instance, the elastic region shows uniform deformation without any local collapse of

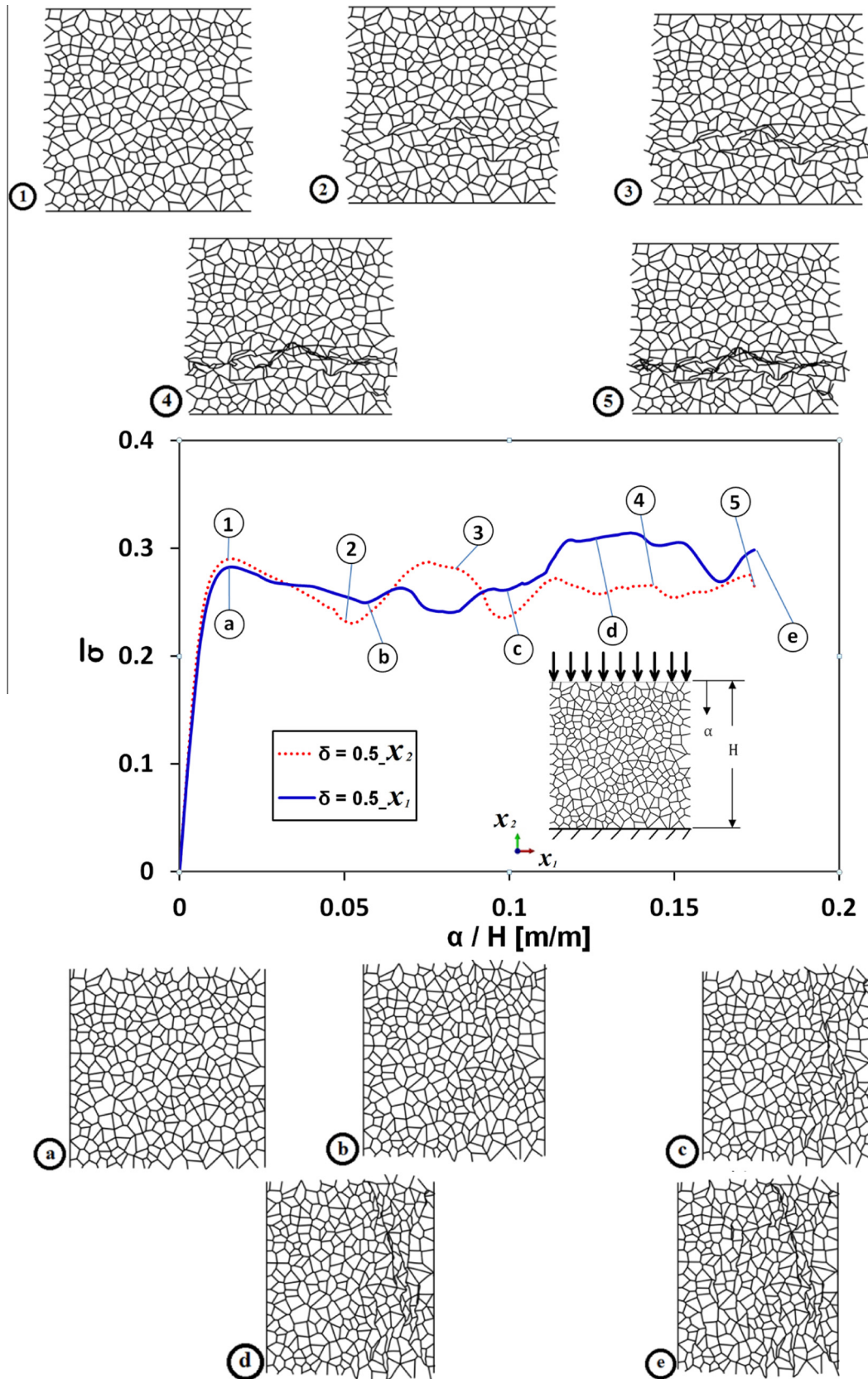


Fig. 5. Normalized stress–strain curves for a 9% Al Voronoi honeycomb with regularity $\delta = 0.5$.

cells. Subsequently, at a certain strain, a softening effect can be observed. This, however, does not necessarily imply a local collapse in the structure. As the simulation progresses, the weakest cell

collapses and the cells located along the weakest path follow the trend. For compression in the x_2 -direction, the collapse path tends to be nearly horizontal but not straight as in the regular honeycomb

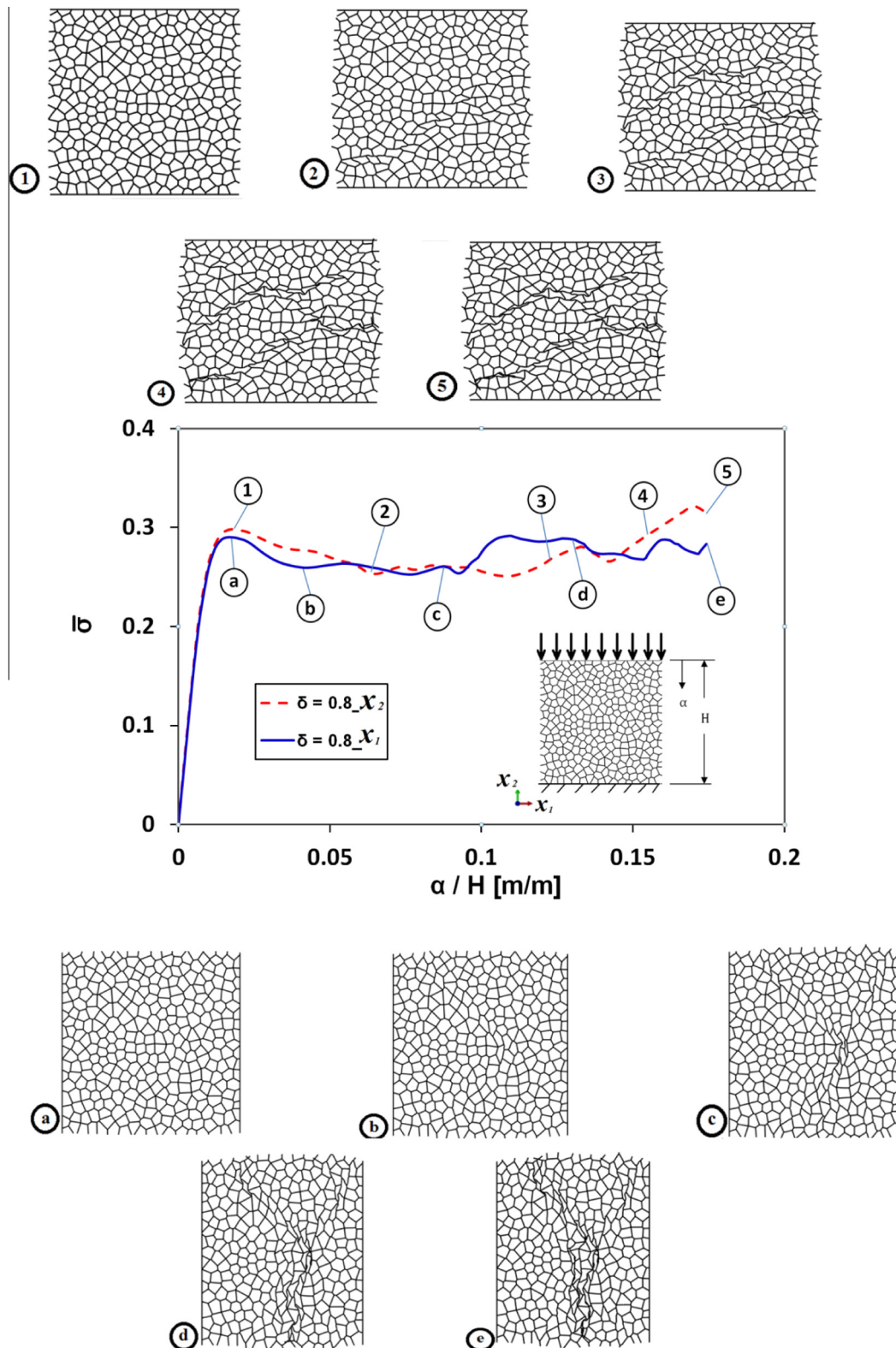


Fig. 6. Normalized stress–strain curves for a 9% Al Voronoi honeycomb with regularity $\delta = 0.8$.

case (Fig. 4). The interaction among the cells successfully prevents interpenetration of nodes once the opposing walls touch each other. Subsequently, the deformation starts to localize next to the original path although evolution of independent paths can also occur as evident in Fig. 6(5). These quasi-isotropic behaviors in the elastic

range have also been observed in all the configurations, namely, $\delta = \{0, 0.5, 0.7, 0.8, 1\}$ with $\bar{\rho} = \{3\%, 5\%, 7\%, 9\%$. These results are not shown for the sake of brevity, but the main properties such as elastic modulus and plastic collapse strength are presented in Sections 4.3 and 4.4.

4.2. Effect of cellular arrangement at a constant regularity

Different arrangement of cells at a fixed regularity parameter (δ) requires generating different sets of nuclei in different trials of the SSI process. Each time the SSI algorithm is executed, it generates a different random arrangement of nuclei even though the regularity and number of nuclei is the same. Its effect on the stress–strain response was studied and the results are presented in Fig. 7 for a representative case of $\delta = 0.8$. Note that the two arrangements including the one in Fig. 6 were studied. As can be seen in Fig. 7, the effect of generating two different geometric configurations using different sets of nuclei but with the same regularity does not have an appreciable effect on the elastic modulus or the plateau strength despite differences in the local oscillations due to cell morphology dissimilarities. That is, the additional arrangement of points produces a new but comparable response in both the elastic and plateau (plastic) regions.

4.3. Role of regularity in 2D

In this section the influence of regularity on the compression response of Voronoi honeycombs is presented. Analyses were performed on Voronoi honeycombs over a wide range of regularities. Specifically, geometries with $\delta = \{0, 0.5, 0.7, 0.8 \text{ and } 1\}$ and $\bar{\rho} = \{3\%, 5\%, 7\%, 9\%\}$ were studied. The responses were averaged between two orthogonal directions to estimate the anticipated scatter in the reported results since we are dealing with nominally isotropic microstructures. Fig. 8 shows the predicted elastic modulus (normalized by the elastic modulus of the bulk material) as a function of the regularity parameter for different relative densities. It suggests an inverse relationship between the regularity and stiffness of the honeycomb. Consequently, highly irregular Voronoi honeycombs have higher values of elastic modulus when compared to their regular counterparts. Silva et al. (1995), Zhu et al. (2001) have also suggested that irregular 2D Voronoi honeycombs are stiffer than the regular honeycombs. Silva et al. (1995) compare the elastic response of irregular honeycombs with the regular ones although they limit the comparison to structures with an invariant regularity parameter and regular ($\delta = 1$) ones. Since Silva et al., have not identified the level of regularity used in their analysis, the range of δ is estimated to be in the range 0.7–0.8. In the present work, the difference in terms of elastic modulus between honeycombs with $\delta = 0.7$ and $\delta = 1$ is approximately 8% whereas Silva et al., found a difference of about 6%. However, a broader range of values of δ suggests a considerable increase of elastic modulus

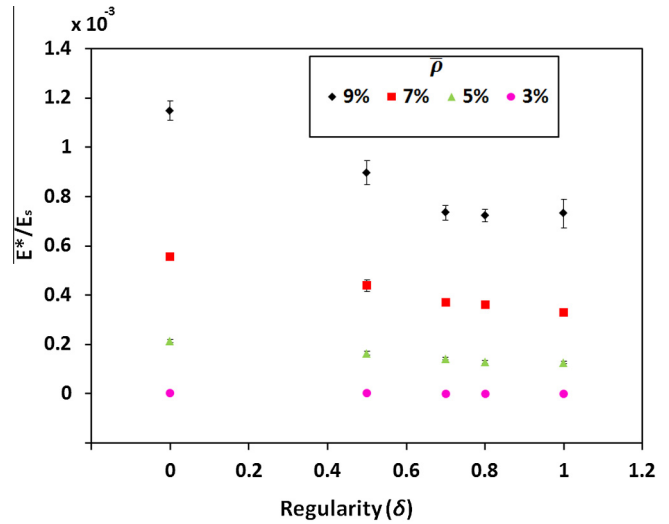


Fig. 8. Effect of regularity on elastic modulus of Voronoi honeycombs of different relative densities.

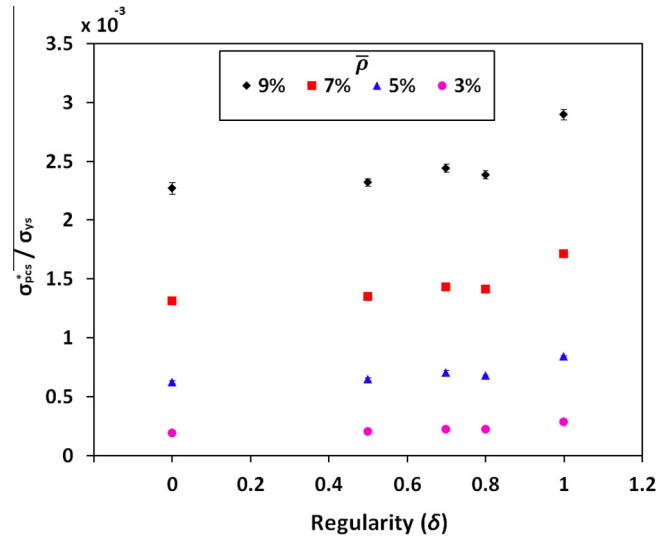


Fig. 9. Effect of regularity on plastic-collapse strength of Voronoi honeycombs for different relative densities.

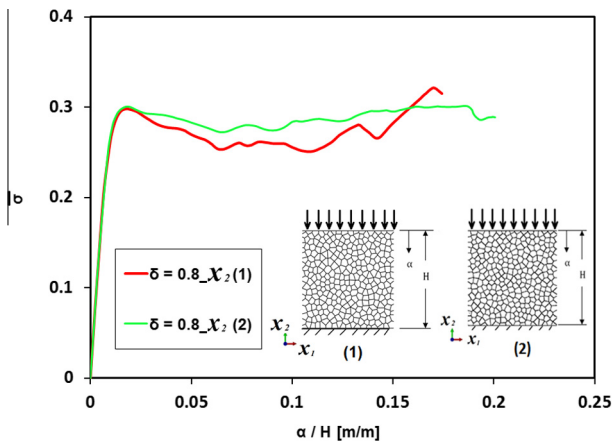


Fig. 7. Aluminum Voronoi honeycomb stress–strain responses with $\bar{\rho} = 9\%$ and $\delta = 0.8$. The results corresponds to two different configurations ((1) and (2)) generated in different trials of the SSI process with the same regularity parameter.

Table 4.1

Elastic modulus data fitting for Voronoi honeycombs with different regularities to determine C_1 .

Regularity	C_1	Coefficient of determination
0	1.587	0.9993
0.5	1.241	0.9993
0.7	1.023	0.9975
0.8	1.003	0.9988
1	0.996	0.9995

for Voronoi honeycombs when regularity is lower than $\delta = 0.7$. The data also suggests that a fully irregular Voronoi honeycomb ($\delta = 0$) is approximately 66% stiffer than a regular counterpart.

The plastic-collapse strength increases with regularity as evident in Fig. 9. This trend is opposite to the one seen in case of the elastic modulus. The plastic-collapse strength of regular honeycombs is approximately {28%, 31%, 35% and 50%} higher than a fully irregular honeycombs for relative densities of $\bar{\rho} = \{9\%, 7\%$,

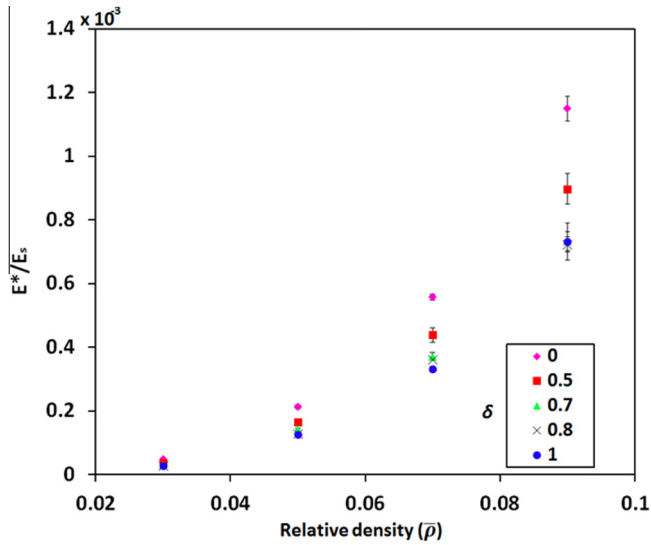


Fig. 10. Variation of elastic modulus of Voronoi honeycombs with relative density for different regularities.

Table 4.2

Plastic-collapse strength data fitting for Voronoi honeycombs with different regularities to determine C_2 .

Regularity	C_2	Coefficient of determination
0	0.2741	0.9955
0.5	0.2814	0.9967
0.7	0.2972	0.9979
0.8	0.2909	0.9981
1	0.3538	0.9988

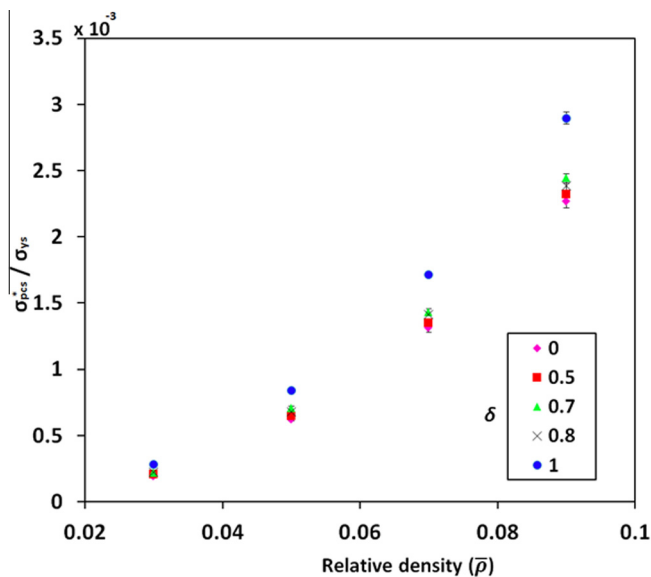


Fig. 11. Plastic-collapse strength of Voronoi honeycombs of different relative densities at different cell regularities.

5%, 3%), respectively. For plastic-collapse strength, the trend is relatively constant between $\delta = 0$ and $\delta = 0.8$ with a considerable enhancement in the range $\delta = 0.8$ to $\delta = 1$.

In light of the elastic modulus and plastic collapse strength variations discussed above, there appears to be a clear trade-off

between the two characteristics when regularity of the cellular structure is varied and hence could be of significance in the design process.

4.4. The effect of relative density on Voronoi honeycombs

The numerical simulations have shown that the reduction of the elastic modulus scales with $(\rho^*/\rho_s)^3$ (Gibson and Ashby, 1997; Gibson et al., 2010; Guo and Gibson, 1999). Accordingly, by fitting the data for elastic modulus variation for different regularities with relative density to a function of the form,

$$\frac{E^*}{E_s} = C_1 \left(\frac{\rho^*}{\rho_s} \right)^3 \quad (5)$$

where E^* is the elastic modulus of the honeycomb, E_s is the elastic modulus of the bulk material. Thus evaluated values of C_1 are tabulated in Table 4.1.

In light of this, it is important to recognize that the constant C_1 depends on the level of regularity in case of Voronoi honeycombs. It should be noted that the Eq. (5) is only applicable to 2D structures whereas for 3D open cell configurations the elastic modulus is shown to vary with the square of the relative density (Gibson et al., 2010; Roberts and Garboczi, 2002). Fig. 10 presents the variation of the normalized elastic modulus of the Voronoi honeycombs with relative density for different regularities.

Similarly, the plastic-collapse strength can be described by an expression of the form (Gibson and Ashby, 1997; Gibson et al., 2010),

$$\frac{\sigma_{pcs}^*}{\sigma_{ys}} = C_2 \left(\frac{\rho^*}{\rho_s} \right)^2 \quad (6)$$

where C_2 is a constant of proportionality, σ_{pcs}^* is the plastic-collapse strength of the honeycomb, σ_{ys} is the yield stress of the bulk material. Table 4.2 tabulates the evaluated values of C_2 for different regularities.

Again, it can be seen that the constant C_2 varies with the level of regularity of the Voronoi honeycombs. It should be noted that, Eq. (6) is only applicable for 2D structures and a new set of equations would be necessary for the 3D counterparts. Fig. 11 presents the simulated variation of the normalized plastic-collapse strength as a function of the relative density for different regularities.

5. Conclusions

In this paper, the role of cellular morphology of structural honeycombs on their compression response has been studied. Of particular interest to the study is the effect of cell regularity and relative density on the elastic–plastic behavior of random and regular honeycombs. Finite element analyses using Timoshenko beam elements and solid modeling methods were developed for this purpose. The Voronoi tessellation technique in 2D was implemented to represent random honeycombs. The representation was able to capture a majority of characteristics observed in natural honeycombs although the surface tension effects which influence geometry of natural honeycombs were not accounted for. The advances and accessibility of additive manufacturing methods motivated this study since Voronoi honeycombs can be directly fabricated from CAD models developed in a virtual environment. For example, this opens the possibility of fully controlling the morphology of cellular structures during production of porous scaffolds. Further, morphological characteristics such as regularity, cross-sectional shape of ligaments, polydispersity of cells and macroscopic shape which cannot be controlled in conventional methods can be fully defined using solid modeling and additive manufacturing techniques.

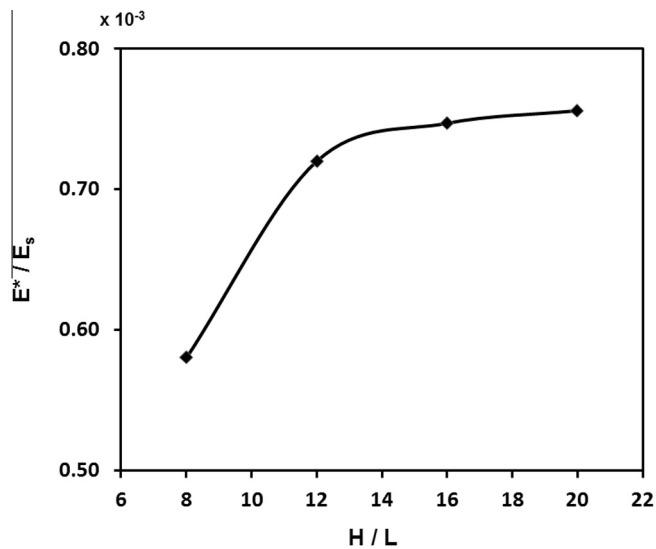


Fig. A1. Convergence of normalized elastic modulus of the cellular structure with the number of cells used in the model. (H : model size, L : cell size).

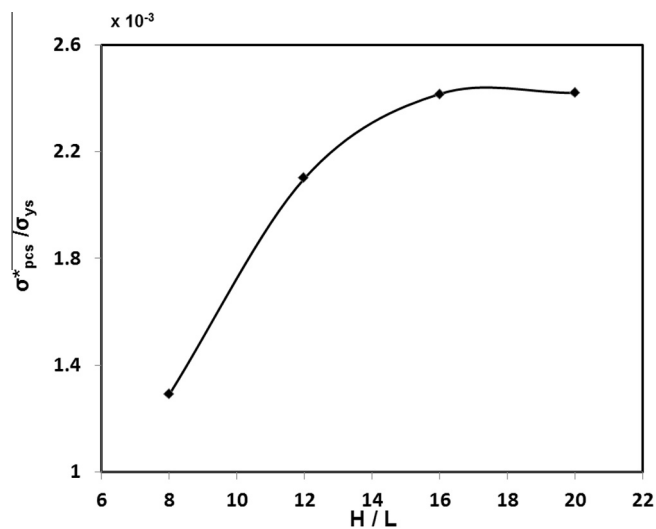


Fig. A2. Convergence of normalized plastic collapse strength of the cellular structure with the number of cells used in the model. (H : model size, L : cell size).

The influence of cell regularity and relative density was studied in Voronoi honeycombs. A nominally isotropic response in the whole range of strains analyzed was observed for the Voronoi honeycombs (with $\delta \neq 1$). That is, the sensitivity of stress–strain responses to the arrangement of cells at a constant regularity parameter was found to be negligible. On the other hand, the regularity parameter was found to have a significant influence not only on the cellular morphology but also the mechanical response. The effect of cell randomness was studied over a wide range of regularity parameters, from fully irregular configurations ($\delta = 0$) to fully regular ones ($\delta = 1$). A Simple Sequential Inhibition (SSI) process was used to create honeycombs with regularities $\delta \leq 0.8$ whereas a fully regular arrangement of hexagonal cells (as a special case of a Voronoi honeycomb with $\delta = 1$) was generated by directly placing the nuclei at a uniform maximum distance of inhibition. An inverse relation was found to exist between the cell regularity and elastic modulus of Voronoi honeycombs, consistent with the previous works. However, the differences between the elastic modulus of random and regular honeycombs was appreciable and much more significant than reported previously. A fully irregular Voronoi honeycomb ($\delta = 0$) was found approximately 66% stiffer than a

regular counterpart. This was attributed to the fact that the cellular structures generated in the present work cover a wider range of regularity parameters. The plastic-collapse strength, on the other hand, showed a direct relationship with cell regularity. The plastic-collapse strength of regular ($\delta = 1$) honeycombs was {28%, 31%, 35% and 50%} higher than a fully irregular ($\delta = 0$) counterpart for relative densities of $\bar{\rho} = \{9\%, 7\%, 5\%, 3\%$, respectively. Regarding the dependency on the relative density of honeycombs, the data suggests that the elastic modulus of Voronoi honeycombs scale with $\bar{\rho}^3$ whereas the plastic-collapse strength and plateau strength scale with $\bar{\rho}^2$. However, the proportionality constants relating the property with the relative density vary with regularity.

Appendix A

The effect of the number of cells was studied in specimens with $\delta = 0.8$ and relative density of 9% where the ratio of the control area to the cell size was equal to $H/L = \{8, 12, 16 \text{ and } 20\}$. Here H and L are the height and average cell size of the specimen. Fig. A1 shows the effect the normalized specimen size has over the normalized elastic modulus. Similarly, Fig. A2 depicts the variation of normalized plastic-collapse strength when H/L ratio was varied. From Figs. A1 and A2, it is clear that the number of cells used in the simulation has a significant effect on the predicted mechanical properties, more so in case of the plastic collapse strength. Further, both the characteristics increase with an increasing normalized specimen size. The normalized elastic modulus attains a plateau corresponding to a H/L ratio of ~ 12 . The normalized plastic collapse strength on the other hand stabilized at a H/L ratio of ~ 16 .

References

- Alkhader, M., Vural, M., 2008. Mechanical response of cellular solids: role of cellular topology and microstructural irregularity. *Int. J. Eng. Sci.* 46, 1035–1051.
- Aluminum Association, I., 2001. <<http://www.matweb.com/search/datasheet.aspx?matguid=4303c5b908ff4cbd91a02fed7d4e8202&ckck=1>>.
- Barber, C.B., Dobkin, D.P., Huhdanpaa, H.T., 1996. The Quickhull algorithm for convex hulls. *ACM Trans. Math. Software* 22, 469–483.
- Boots, B.N., 1982. The arrangement of cells in “random” networks. *Metallography* 15, 53–62.
- Borel, É., 1913. Mécanique statistique et irréversibilité. *J. Phys.* 3, 189–196.
- Cricri, G., Perrella, M., Cali, C., 2013. Honeycomb failure processes under in-plane loading. *Compos. B Eng.* 45, 1079–1090.
- Da Silva, A., Kyriakides, S., 2007. Compressive response and failure of balsa wood. *Int. J. Solids Struct.* 44, 8685–8717.
- Gaitanaros, S., Kyriakides, S., Kraynik, A.M., 2012. On the crushing response of random open-cell foams. *Int. J. Solids Struct.* 49, 2733–2743.
- Gan, Y.X., Chen, C., Shen, Y.P., 2005. Three-dimensional modeling of the mechanical property of linearly elastic open cell foams. *Int. J. Solids Struct.* 42, 6628–6642.
- Gibson, L.J., Ashby, M.F., 1997. Cellular solids: structures & properties. In: Series C.S.S.A. second ed., Cambridge University Press, New York.
- Gibson, L.J., Ashby, M.F., Harley, B.A., 2010. Cellular Material in Nature and Medicine. Cambridge University Press, New York.
- Gong, L., Kyriakides, S., 2005. Compressive response of open cell foams Part II: initiation and evolution of crushing. *Int. J. Solids Struct.* 42, 1381–1399.
- Gong, L., Kyriakides, S., Jang, W.Y., 2005. Compressive response of open-cell foams. Part I: morphology and elastic properties. *Int. J. Solids Struct.* 42, 1355–1379.
- Guo, X.E., Gibson, L.J., 1999. Behavior of intact and damaged honeycombs: a finite element study. *Int. J. Mech. Sci.* 41, 85–105.
- Hibbitt, K.S. Inc, 2002. ABAQUSTM User’s Manual (version 6.3).
- Jang, W.-Y., Kyriakides, S., 2009. On the crushing of aluminum open-cell foams: Part I. Experiments. *Int. J. Solids Struct.* 46, 617–634.
- Jang, W.-Y., Kraynik, A.M., Kyriakides, S., 2008. On the microstructure of open-cell foams and its effect on elastic properties. *Int. J. Solids Struct.* 45, 1845–1875.
- Jhaver, R., 2009. Thesis-compression response and modeling of interpenetrating phase composites and foam-filled honeycombs. Mechanical Engineering, Auburn, Auburn.
- Klein, R., 1989. Concrete and Abstract Voronoi Diagrams. Springer-Verlag.
- Liu, C., Xia, Z., Czernuszka, J.T., 2007. Design and development of three-dimensional scaffolds for tissue engineering. *Chem. Eng. Res. Des.* 85, 1051–1064.
- Liu, Y.D., Yu, J.L., Zheng, Z.J., Li, J.R., 2009. A numerical study on the rate sensitivity of cellular metals. *Int. J. Solids Struct.* 46, 3988–3998.
- Martinez, W.L., Martinez, A.R., 2002. Computational Statistics Handbook with MATLAB. Chapman & Hall/CRC.
- Moller, J., 1994. Lectures on Random Voronoi Tessellations. Springer-Verlag.

- Okabe, A., Boots, B., Sugihara, K., Chiu, S.N., 1945. *Spatial Tessellations: Concepts and Applications of Voronoi Diagrams*, second ed. John Wiley & Sons Ltd.
- Papka, S.D., Kyriakides, S., 1994. In-plane compressive response and crushing of honeycomb. *J. Mech. Phys. Solids* 42, 1499–1532.
- Papka, S.D., Kyriakides, S., 1998. Experiments and full-scale numerical simulations of in-plane crushing of a honeycomb. *Acta Mater.* 46, 2765–2776.
- Roberts, A.P., Garboczi, E.J., 2002. Elastic properties of model random three-dimensional open-cell solids. *J. Mech. Phys. Solids* 50, 33–55.
- Silva, M.J., Gibson, L.J., 1997. Effects of non-periodic microstructure and defects on the compressive strength of two-dimensional cellular solids. *Int. J. Mech. Sci.* 39, 549–563.
- Silva, M.J., Hayes, W.C., Gibson, L.J., 1995. The effects of non-periodic microstructure on the elastic properties of two-dimensional cellular solids. *Int. J. Mech. Sci.* 37, 1161–1177.
- Tekoglu, C., Gibson, L.J., Pardoan, T., Onck, P.R., 2011. Size effects in foams: experiments and modeling. *Prog. Mater. Sci.* 56, 109–138.
- Zhu, H.X., Hobdell, J.R., Windle, A.H., 2000. Effects of cell irregularity on the elastic properties of open-cell foams. *Acta Mater.* 48, 4893–4900.
- Zhu, H.X., Hobdell, J.R., Windle, A.H., 2001. Effects of cell irregularity on the elastic properties of 2D Voronoi honeycombs. *J. Mech. Phys. Solids* 49, 857–870.
- Zhu, H.X., Thorpe, S.M., Windle, A.H., 2006. The effect of cell irregularity on the high strain compression of 2D Voronoi honeycombs. *Int. J. Solids Struct.* 43, 1061–1078.